

1 Morpho-functional experience-dependent plasticity in the honeybee brain

2 Mara Androne^{1 *}, Benjamin F. Timberlake¹, Giorgio Vallortigara¹, Renzo Antolini^{2,1}, and
3 Albrecht Haase^{2,1 *}

4 1 Center for Mind/Brain Sciences, University of Trento, Rovereto, Italy

5 2 Department of Physics, University of Trento, Trento, Italy

6
7 *Correspondence to

8 albrecht.haase@unitn.it

9 mara.androne@unitn.it

10
11
12 Manuscript is published:

13 Androne, M., Timberlake, B.F., Vallortigara, G., Antolini, R., and Haase, A. 2017. Morphofunctional
14 experience-dependent plasticity in the honeybee brain. Learn Mem. 24:622–629.

15 online at <http://www.learnmem.org/cgi/doi/10.1101/lm.046243.117>.

22 Abstract

23 Repeated or prolonged exposure to an odorant without any positive or negative reinforcement
24 produces experience-dependent plasticity, which results in habituation and latent inhibition. In the
25 honeybee (*Apis mellifera*), it has been demonstrated that, even if the absolute neural
26 representation of an odor in the primary olfactory center, the antennal lobe (AL), is not changed by
27 repeated presentations, its relative representation with respect to unfamiliar stimuli is modified. In
28 particular, the representation of a stimulus composed of a 50:50 mixture of a familiar and a novel
29 odorant becomes more similar to that of the novel stimulus after repeated stimulus pre-exposure.
30 In a calcium imaging study, we found that the same functional effect develops following prolonged
31 odor exposure. By analyzing the brains of the animals subjected to this procedure, we found that
32 such functional changes are accompanied by morphological changes in the AL (*i.e.* a decrease in
33 volume in specific glomeruli). The AL glomeruli that exhibited structural plasticity also modified their
34 functional responses to the three stimuli (familiar odor, novel odor, binary mixture). We suggest a
35 model in which rebalancing inhibition within the AL glomeruli may be sufficient to elicit structural
36 and functional correlates of experience-dependent plasticity.

37

38 Introduction

39 The primary olfactory-processing center in the brain of the honeybee *Apis mellifera*, the antennal
40 lobe (AL), is known to undergo functional plasticity changes in response to specific olfactory
41 experiences. Classical appetitive conditioning has been extensively investigated for its potential to
42 modify the representation of the rewarded odor in the AL (Sandoz 2011; Giurfa and Sandoz 2012).
43 A number of calcium imaging studies led to contradictory results (Faber et al. 1999; Sandoz et al.
44 2003; Peele et al. 2006; Hourcade et al. 2009; Denker et al. 2010) until it became clear that such
45 changes are not absolute, but relative to the representation of non-rewarded odors (Faber et al.
46 1999; Rath et al. 2011). Thus, in accord with associative learning, the AL would act as a filter,
47 increasing the relative salience of the rewarded odor pattern with respect to other stimuli. The

48 resulting pattern would then be conveyed to higher brain areas, where the odor's valence is
49 evaluated and behavioral responses are triggered (Chen et al. 2015). The reverse would happen in
50 cases of non-associative learning (Locatelli et al. 2013; Chen et al. 2015): an odor that is
51 repeatedly presented to the bee olfactory system, associated with neither positive nor negative
52 reinforcement, would lose relevance to the animal. The AL filter would reduce the relative salience
53 of this odor response pattern with respect to others. In summary, following associative learning,
54 previously rewarded components will have a competitive advantage in odor mixture representation
55 over unrewarded ones, while, in the case of non-associative learning, novel components will have
56 an advantage over familiar ones (Locatelli et al. 2013; Chen et al. 2015). As a result, in non-
57 associative learning the pre-exposed stimulus becomes less likely to affect behavior, e.g. leading
58 to overshadowing effects (Locatelli et al. 2013). In the case of prolonged rather than repeated
59 exposure, in the fruit fly *Drosophila melanogaster*, a diminished olfactory avoidance of a previously
60 habituated aversive odorant was observed (Manning 1967; Devaud et al. 2001; Sachse et al. 2007;
61 Das et al. 2011). All these effects have been shown to be caused by an enhancement of inhibitory
62 inputs from local neurons (LNs) to projection neurons (PNs) within the AL (Sachse et al. 2007; Das
63 et al. 2011; Locatelli et al. 2013; Chen et al. 2015). In the case of associative learning, the relative
64 increase in salience of the neural representation of the rewarded odor is due to octopamine-based
65 modulation of LN activity (Sinakevitch et al. 2013; Chen et al. 2015). In the case of non-associative
66 experiences and habituation, the relative decrease in odor salience is dependent on recurrent
67 inhibition on PNs via LNs (Sudhakaran et al. 2012). In the honeybee, both repeated (Chandra et al.
68 2010) and prolonged (Fernández et al. 2009) presentations of an unreinforced odor can produce
69 latent inhibition, i.e. a delay in the acquisition of an associative memory of the same odor
70 (Fernandez et al. 2012). Latent inhibition has been suggested to rely on serotonin transmission
71 (Fernandez et al. 2012). Therefore, this neurotransmitter might also be involved in the mechanisms
72 of "habituation", "activity-dependent plasticity", or "central adaptation" previously described
73 (Devaud et al. 2001; Sachse et al. 2007; Das et al. 2011). However, the site of action of serotonin
74 responsible for latent inhibition was not precisely localized within the bee brain (Fernandez et al.

2012). In the fruit fly, functional plasticity related to odor exposure was shown to be accompanied by volumetric changes at defined locations within the AL (Sachse et al. 2007; Das et al. 2011). These changes are believed to arise from increased branching and greater synaptic contact between LNs and PNs within the glomeruli (Sachse et al. 2007; Das et al. 2011). On the contrary, decreased glomerular volumes, observed in one study following odor exposure, were ascribed to synaptic loss (Devaud et al. 2001). Olfactory receptor neurons (ORNs), whose axons also contribute to glomerular connectivity, were shown in both cases to be morphologically and functionally unchanged by the procedure (Devaud et al. 2001; Sachse et al. 2007). In the honeybee, volumetric changes of specific AL glomeruli have been described in relation to age and foraging experience (Winnington et al. 1996; Sigg et al. 1997; Brown et al. 2004), or following associative learning — either at an early age (Arenas et al. 2012) or in foragers (Hourcade et al. 2009). However, structural plasticity related to non-associative experiences within the AL has not yet been reported. Here, we investigated the effects of prolonged odor exposure on AL glomerular volumes collected via two-photon microscopy (Haase et al. 2010) and then tried to correlate the observed anatomical changes with functional modifications, observed via calcium imaging.

90

91 Results

92 To induce experience-dependent plasticity, bees were divided into three groups and pre-exposed
93 over 3 days to one of two floral odorous compounds, 1-hexanol (HEX) and 1-nonanol (NNL), or to
94 mineral oil as a stimulus control (CTR; for details see Materials and Methods section). At the end of
95 the 72h-procedure, a subset of bees was injected in their PNs with the calcium sensor fura-2 and
96 then kept overnight for another 18h in the pre-exposure tents. The day after, stimulus-evoked
97 activity was evaluated in a calcium-imaging experiment, in which each animal was presented with
98 the single odors HEX and NNL and a binary 50:50 mixture (MIX). The change in fluorescence over
99 time was analyzed for several glomeruli in $n = 5$ bees of the HEX pre-exposed group, $n=4$ bees of
100 the NNL pre-exposed group, and $n = 5$ control bees. A subset of glomeruli was unambiguously

101 identified within each bee. The activity patterns were averaged for single glomeruli over all
 102 individuals in which they could be identified within the three pre-exposure groups. These average
 103 glomerular response patterns show clear deviations among groups (Fig. 1). Recordings were
 104 limited to a single focal plane in each bee, to avoid odor over-exposure by excessive repetition of
 105 the same paradigm of stimulation. Due to deviations among these focal planes in different animals,
 106 glomerular subsets were not fully overlapping across different bees. Moreover, some glomeruli
 107 within each recording could not be identified with full certainty. Therefore, recorded data contained
 108 more information than those shown in Fig. 1. To exploit the full glomerular response profile in each
 109 animal for further analysis, instead of averaging identified glomeruli only, glomeruli of all bees of
 110 the same treatment were pooled together to construct overall odor representations in each group
 111 ($n_{\text{CTR}} = 56$, $n_{\text{HEX}} = 62$, $n_{\text{NNL}} = 44$). The dimensionality of this coding space was then reduced by
 112 principal component analysis (PCA). The odor-response dynamics (1 s during stimulus and 1 s
 113 post-stimulus) are shown in the first two principal components (Fig. 2). The PCA shows a relative
 114 difference in odor representation among the three pre-exposed groups. In the CTR group, the
 115 binary mixture MIX activation vector is centered between the two pure components HEX and NNL,
 116 while in the odor pre-exposed groups, MIX shifts away from the familiar compound and toward the
 117 novel odor. This effect can be quantified by the Euclidean distance (ED) between odor pairs in the
 118 individual groups. The EDs were calculated based on the average activity of the recorded glomeruli
 119 in the interval 200 to 400 ms after stimulus onset. We normalized the EDs within each group to the
 120 ED between the pure compounds (Fig. 3A). In the CTR group, in which animals were exposed to
 121 mineral oil only, single odors are again shown to be equidistant from the 50:50 mixture, while in the
 122 odor-pre-exposed groups, the ED between mixture and novel odor is reduced. However, this
 123 difference was significantly different from zero only in the case of NNL pre-exposed bees (z-test of
 124 sampling distribution of differences, $p = 0.016$; Fig. 3A, right).

125 To compare this relative shift among groups, we computed ratios

$$126 \quad (ED_{\text{HEX_MIX}} - ED_{\text{NON_MIX}}) / (ED_{\text{HEX_MIX}} + ED_{\text{NON_MIX}}) \quad (1)$$

127 within each group (Fig. 3B). This ratio was found to be approximately zero in the case of CTR
128 bees, while it increased for HEX pre-exposed bees and decreased for NNL pre-exposed bees. The
129 difference between the two pre-exposed groups was significant (z-test of sampling distribution of
130 differences, $p = 0.041$; Fig. 3B).

131 Since odor exposure continued over several days, we asked whether the observed functional
132 plasticity was accompanied by structural changes. Therefore, following a fluorescent
133 immunolabelling procedure of the synaptic compartments, brain morphology was imaged and
134 analyzed for a subset of animals from each treatment group, sacrificed at the end of the 72h-
135 exposure period. The AL glomeruli were identified, segmented, and 3D-reconstructed. A subset of
136 glomeruli was bilaterally measured in each individual. The chosen glomeruli were selected for
137 responding strongly either to HEX (glomeruli T1-38 and T1-28), to NNL (glomeruli T1-17 and T1-
138 33) or to neither in particular (glomeruli T1-47 and T1-42), (see response maps in Fig. 1).

139 Measured glomerular volumes are reported in Fig. 4. A mixed ANOVA was performed, with
140 right/left side and glomerulus number as within-subject factors and treatment as between-subject
141 factor. Treatment, glomerulus, and their interaction significantly affected volumes (Treatment: $F_{2,40}$
142 $= 7.8$, $p = 0.0014$; Glomerulus: $F_{5,200} = 450$, $p < 10^{-106}$; Treatment*Glomerulus: $F_{10,200} = 3.0$, $p =$
143 0.0017). Brain side did not show any significant main effect or interaction with the other factors
144 (Side: $F_{1,40} = 0.060$, $p = 0.81$; Treatment*Side: $F_{2,40} = 1.4$, $p = 0.26$; Glomerulus*Side: $F_{5,200} = 0.29$, p
145 $= 0.92$; Treatment*Glomerulus*Side: $F_{10,200} = 0.80$, $p = 0.63$), meaning that the volumetric changes
146 we observed were not lateralized (Rigosi et al. 2011; Haase et al. 2011; Frasnelli et al. 2014).

147 Accordingly, for further independent sample *t*-test comparisons, corresponding right and left
148 glomeruli were averaged in each bee. Odor exposure led to a decrease in volume of specific
149 glomeruli. In particular, glomeruli T1-33 and T1-17 were both reduced in cases of NNL pre-
150 exposure. A non-significant trend was also observed for a reduction in T1-28 volume in HEX pre-
151 exposed bees.

152 Based on the observation that glomeruli T1-33 and T1-17 were most changed by odor pre-
153 exposure, their single odor-evoked response profiles were compared among groups (Fig. 5). T1-17

154 response profiles to the three stimuli HEX, NNL, and MIX are shown in Fig. 5A; those of T1-33, in
155 Fig. 5B. Parts of the response pattern clearly changed following olfactory pre-exposure. In the CTR
156 group (green bars), neither glomerulus responded to HEX (Fig. 5A, B left), but both were strongly
157 excited by NNL (Fig. 5A, B center) and the MIX (Fig. 5A, B right). Glomeruli in the HEX pre-
158 exposure group (red bars) developed a slightly inhibitory response to HEX, although not
159 significantly (Fig. 5A, B left). At the same time, the responses to NNL (Fig. 5A, B middle) and to the
160 MIX (Fig. 5A, B right) increased in comparison to those of CTR bees (significantly in the case of
161 glomerulus T1-33). Responses of the NNL pre-exposed group (yellow bars) showed slight changes
162 in the opposite direction. The two pre-exposure groups gave rise to significantly different response
163 to both NNL and MIX in the case of glomerulus T1-33 and to MIX in the case of glomerulus T1-17.

164

165 Discussion

166 We used a paradigm of prolonged pre-exposure of honeybees to single-odor compounds, similar
167 to those that have been shown to produce measurable morphological and functional changes in
168 *Drosophila melanogaster* (Devaud et al. 2001; Sachse et al. 2007; Das et al. 2011). In the
169 honeybee, repeated short stimulation with a single odorant induces a change in the relative
170 representation of the binary mixture composed of this odor and a novel compound (Locatelli et al.
171 2013). Although our bees were treated instead with a continuous, long-term pre-exposure,
172 functional imaging revealed the same effect, *i.e.* a suppression of the exposed odor representation
173 in the odor response code of the mixture. This confirms the results of Locatelli *et al.* (Locatelli et al.
174 2013) and shows that experience-dependent plasticity occurs in the honeybee not only during
175 repeated exposure, but also during long-term exposure, as applied in our experiment. Interestingly,
176 the latent inhibition of the proboscis extension response conditioning, a well-known consequence
177 of unreinforced odor exposure in the honeybee, appears in cases of both repeated (Chandra et al.
178 2010) and prolonged (Fernández et al. 2009) odor exposure. On the other hand, we would exclude
179 mechanisms of associative learning, as the paradigm of odor pre-exposure was specifically
180 designed to avoid a spatial and completely synchronized temporal overlap between the two stimuli

(odor, sucrose reward), *i.e.* besides being placed at opposite locations within the tents, the odor had no specific anticipatory value with respect to the sucrose. In fact, even if most of the time both stimuli were present, animals could experience periods with either only the odor or only the sucrose reward. Moreover, when the onset of the odor stimulus was preceding that of the sucrose reward, the inter-stimulus interval (ISI) was at least 1 hour, well past any suggested time scale for associative learning (Matsumoto et al. 2012).

Recently, Chakroborty and colleagues reported on changes in PN activity following 30 min adaptation of the olfactory system through exposure to complex mixtures (Chakroborty et al. 2016). In our experiments, a long-duration pre-exposure was used to study the so-far-unaddressed issue of structural plasticity in relation to unrewarded odor exposure, which requires longer timescales. The literature on prolonged odor exposure in *Drosophila*, suggests that odor-specific volumetric changes in the glomeruli would happen only during a certain time window following eclosion (Devaud et al. 2003). However, we observed structural plasticity in adult forager bees, well past any such window. The high flexibility that foraging activity requires, regarding individuation of food sources in space and time, may account for the preservation of plasticity in the honeybee olfactory structures.

Volumetric changes in the AL glomeruli have been reported in the adult bee alongside associative learning (Hourcade et al. 2009; Arenas et al. 2012). Here, we report, for the first time, volumetric changes accompanying unrewarded odor exposure. Our volumetric measurements on reconstructed glomeruli show significant changes in two of the six sampled glomeruli (T1-33 and T1-17) for one of the two pre-exposure odors (NNL). Adult activity-dependent plasticity, therefore, is able to produce similar volumetric changes irrespective of foraging experience before the experiment. It is likely that effects would be even stronger under experience- and age-controlled conditions.

The functional changes in those glomeruli showing structural plasticity (T1-17 and T1-33) suggest that the overall effects of unrewarded odor exposure on the odor code (Locatelli et al. 2013) are distributed across different glomeruli. In particular, we found significant differences in the response

208 of glomeruli T1-17 and T1-33 to the binary mixture in the two pre-exposure groups. Moreover,
209 trends can be observed, such as a slightly inhibitory HEX response for HEX pre-exposed bees in
210 both T1-17 and T1-33, and a slight excitatory response to HEX in T1-33 for NNL pre-exposed
211 bees. However, larger n would be required to confirm these non-significant trends.

212 Functional effects observed in those two glomeruli, could be summarized the following way: the
213 tuning of the T1-17 and T1-33 outputs (PNs), that normally signal NNL, became even sharper in the
214 case of HEX pre-exposure and broader, that is, more accepting to odors other than NNL, - in the
215 case of NNL pre-exposure. Under this point of view, the case of glomerulus T1-17 is particularly
216 interesting: in the CTR group, this glomerulus exhibited an excitatory response to NNL but no
217 response to HEX, so one would expect the response to the binary mixture (MIX) to closely
218 resemble the response to NNL in all groups. However, in the case of NNL pre-exposed bees, the
219 presence of HEX seems to have dampened the response to NNL within the binary mixture, as
220 compared to the response to NNL alone, causing an increase of mixture suppression (Deisig et al.
221 2006). Thus, the HEX component becomes more relevant to the MIX response of this glomerulus,
222 even though in its pure form it did not elicit a response. Considering this, and the slight inhibitory
223 response to HEX in the HEX pre-exposed group (both in T1-17 and T1-33), there seems to be a
224 competition between NNL and HEX stimuli for the output activity of T1-17 and T1-33. This is not
225 surprising, considering the high level of interconnectivity within the AL.

226 It is difficult to hypothesize which mechanism might have produced these shifts in odor response.
227 We would exclude a major role of peripheral sensory adaptation, because the timescale needed for
228 recovering such effect is usually minutes (Zufall and Leinders-Zufall 2000). The only animal in
229 which longer-lasting adaptation was described (3 h) is the nematode *C. elegans* (Colbert and
230 Bargmann 1995). At the time of imaging, our bees had not experienced the odor of pre-exposure
231 since at least 1 h. To our knowledge, such long adaptation recovery time has never been
232 described in an insect.

233 A change in the connectivity of the AL seems the most probable reason for the functional plasticity
234 observed. In particular, comparing functional data to volumetric changes, a modification at the level

235 of ORNs or at the level of LNs can be hypothesized. A reduction of connections from ORNs to
236 glomeruli T1-17 and T1-33 might cause a loss of tuning strength in the case of NNL pre-exposed
237 bees and the reduction in volumes. Even if odor conditioning in the honeybee can modify olfactory
238 receptor (OR) expression in the periphery, non-associative olfactory experience, such as pseudo-
239 conditioning, does not produce the same modifications (Claudianos et al. 2014). To our knowledge,
240 data on prolonged odor exposure and its effect on ORN expression is missing in the honeybee.
241 However, the hypothesis of a changing number or connectivity of ORN would be at odds with
242 findings in *Drosophila*, where number, morphology, and physiology of ORNs were not affected by
243 odor pre-exposure (Devaud et al. 2001; Sachse et al. 2007).
244 Alternatively, a decrease in volume at specific locations can be explained by a decrease in
245 branching and synapses from inhibitory LNs onto PNs. This would be in accordance with results in
246 *Drosophila*, where an enhancement of GABAergic transmission from LNs to active PNs (recurrent
247 inhibition) followed odor pre-exposure (Sachse et al. 2007; Das et al. 2011; Sudhakaran et al.
248 2012). This enhancement, besides causing a volume increase, was necessary and sufficient to
249 cause behavioral habituation (Das et al. 2011). In particular, one *Drosophila* study reported a
250 volumetric increase following odor exposure in those glomeruli that are strongly activated by the
251 pre-exposure odor, alongside with increased inhibition in the response of the same glomeruli to
252 those odors (Sachse et al. 2007). Another study found a volume decrease of glomeruli without
253 clear correlation to their involvement in the odor response (Devaud et al. 2001). We found the
254 same effect in NNL pre-exposed bees in glomeruli T1-17 and T1-33, which are strongly activated
255 by NNL (Fig. 1)
256 However, if a loss of inhibition underlies the volume loss in T1-17 and T1-33 in NNL-exposed bees,
257 our functional results suggest that this favors the transmission of HEX, rather than NNL
258 information. Responses to HEX and NNL in the honeybee are in fact far more distributed across
259 glomeruli than the response to CO₂ in the fruit fly AL (one responsive glomerulus; Sachse and
260 Galizia 2002; Sachse et al. 2007). It might well be that standard ORN input (as in CTR bees) from
261 a HEX stimulus reaches glomeruli T1-17 and T1-33 but is then strongly blocked, rather than

262 passed on, to the advantage of a contribution of NNL. This would be in accordance with a model in
263 which functional inhibition, rather than stochastic or morphological, shapes the responses of PNs
264 to similar odors (Linster et al. 2005). Inputs of ORNs activated by HEX and projecting to different
265 glomeruli would indirectly prevent PNs of T1-33 and T1-17 from responding to the same odor, thus
266 sharpening the response to NNL, as suggested elsewhere (Sachse and Galizia 2002). Similar
267 phenomena are found in *Drosophila* (Silbering and Galizia 2007). This default blocking, or
268 “occlusion”, would be partially lost in our NNL pre-exposed bees, causing the MIX to be
269 represented more similarly to HEX, and accompanied by volume loss in the glomeruli in question.
270 To conclude, we demonstrated that prolonged odor pre-exposure causes functional plasticity,
271 shifting the relative representation of a binary mixture of the pre-exposure odor and a novel odor
272 towards that novel compound. The odor of pre-exposure, losing functional relevance is partially
273 suppressed in the mixture representation that is projected to higher brain centers. We identified
274 single glomeruli causing these changes by measuring absolute differences in the responses to the
275 two odors and their binary mixture, depending on the odor of pre-exposure. We observed for the
276 first time accompanying structural plasticity in these glomeruli, manifested as a decrease in
277 volume. We suggest as an underlying mechanism the loss of inhibition (or “occlusion”) of the novel
278 compound with respect to the pre-exposed odor.

279

280 Materials and Methods

281

282 Animals

283 Forager honeybees were collected with a transparent Plexiglas pyramid at the entrance of the hive
284 in spring and summer 2015.

285

286 Odor pre-exposure

287 The bees were caged in groups of \approx 30-40 individuals in insect tents (BugDorm-2120). The
288 exposure procedure started at 4 p.m. and lasted 72 h. Odorants used were 1-hexanol (HEX) in one

289 tent and 1-nonanol (NNL) in a second enclosure (all odors: 1:50 dilution in mineral oil up to a total
290 volume of 100 μ l). In a third tent, a control group was exposed to mineral oil only (all compounds
291 from Sigma-Aldrich). All odor samples were suffused onto a piece of filter paper, enclosed in a
292 plastic Petri dish with a perforated lid, and set inside each tent. Bees had access to a feeder in the
293 form of a glass Boardman bottle containing 50% sucrose solution seeping up through cylindrical
294 dental filters. The feeder and the odor source were placed spatially separated in opposite corners
295 of the tents (see Supplementary material, Fig. S1). An additional Petri dish carrying pure water was
296 added at a third location to provide drinking water and to keep humidity at a constant level. The
297 tents were kept in a single room at a distance of \approx 3 m and were loosely covered with transparent
298 plastic wrap in order to avoid excessive odor leakage. On the first day, bees were first provided
299 with food and water. The odor dispenser was added after one hour. Each following day, food and
300 odors were removed independently for certain periods, according to a daily schedule shown in Fig.
301 S1, and renewed afterwards. The temperature and humidity of the room were monitored and kept
302 respectively between 22-26 $^{\circ}$ C and 45-55%. Lights were turned on in the morning and off in the
303 evening (see Supplementary material, Fig. S1).

304

305 Functional imaging protocol

306 A subset of bees was prepared for *in vivo* calcium imaging. Briefly, after opening a cuticle window
307 on top of the head, on one side of the brain, dextran-conjugated fura-2 (Thermo Fisher
308 Scientific) was injected into the medial and lateral antenno-cerebral tracts (m- and l-ACTs) (Paoli et
309 al. 2016b) via a pulled borosilicate glass needle. The next day, fluorescence changes in the ALs
310 were recorded while stimulating the animals with 1-hexanol (HEX), 1-nonanol (NNL), and a binary
311 50:50 mixture of the two (MIX). Calcium-dependent fluorescence changes were acquired through
312 repeated scanning (framerate \approx 50 Hz) of a 1D trace crossing all visible glomeruli (\approx 15-20) within
313 one focal plane. This plane was chosen to contain the landmark glomeruli T1-17, T1-33, T1-42. For
314 further details see (Paoli et al. 2017).

315

316 Odor stimuli

317 During measurements, odor stimuli were delivered to the bee antennae through a constant air flow
318 via a custom-made stimulus generator, controlled by a National Instruments board via a LabVIEW
319 interface (Paoli et al. 2016a). The odor stimuli consisted in the head space of glass vials containing
320 HEX diluted 1:500 or NNL diluted 1:250 (due to its lower volatility), both in mineral oil. The binary
321 mixture was created by coherent summation of both individual channels. Each pure odor
322 application had duration of 1 s and was repeated 6 times. The initial delay was 2 s for the novel
323 odor and 8 s for pre-exposed odor. By using stimulus periods of 4 s for the novel odor and 2 s for
324 the pre-exposed odor, a stimulus pattern is created which presents the novel odor, the pre-
325 exposed odor, and the binary mixture in a pseudo-random manner (see Supplementary material,
326 Fig. S2). CTR bees were randomly stimulated with the protocol of either HEX or NNL group.

327

328 Exclusion of biases from different stimulation paradigms in different groups

329 To exclude that the different order of odor presentation and the slightly different inter-stimulus
330 intervals, rather than the pre-exposure procedure cause the different functional responses in the
331 three groups, we compared odor-evoked responses in individual bees subjected to different
332 stimulation paradigms (1 NNL pre-exposed bee, 1 HEX pre-exposed bee, and 2 CTR bees which
333 received one or the other stimulation paradigm) in glomeruli T1-33 (Fig. S3) and T1-17 (Fig. S4).
334 The responses to the MIX diverge between NNL pre-exposed and HEX pre-exposed animals, as
335 we discuss in the Results section. Responses in CTR animals are similar to those of HEX pre-
336 exposed bees (response to MIX = response to NNL), irrespective of the stimulation paradigms.
337 This allows us to exclude major effects of the stimulation paradigm (order of presentation) on the
338 recorded functional patterns.

339

340

341 Functional data analysis

342 Calcium imaging data (fluorescence intensity along the scanline as a function of time) were post-
343 processed using MATLAB (Mathworks). After de-noising via spatial and temporal moving average
344 filtering (Kernel size: 30 $\mu\text{m} \times 100\text{ ms}$), responding regions were assigned to single glomeruli in a
345 semi-automatic algorithm. The temporal signal was then split into single stimulus windows, from
346 0.5 s pre-stimulus to 1 s post-stimulus, for each glomerulus. The relative activation was obtained
347 by normalizing the fluorescence intensity to the pre-stimulus baseline: $-\Delta F/F$. We averaged this
348 signal over the 3 repetitions performed for every stimulus protocol in every subject. Only glomeruli
349 responding with an average stimulus-evoked activity (200-500 ms after stimulus onset) significantly
350 (1.96σ) deviating from the average baseline activity were considered for quantitative analysis of
351 the odor response pattern. The average $-\Delta F/F$ (200-400 ms after stimulus onset) was used as a
352 measure of maximum response. To analyze the separation of the odor response maps in
353 glomerular coding space, the Euclidean distance ED between two odors x and y was calculated:

$$354 \quad ED_{x,y} = \sqrt{\sum_{i=1}^n (x_i - y_i)^2} \quad (2)$$

355 where x_i and y_i are the maximum responses of a single glomerulus i , which are summed over all n
356 glomeruli of all bees in all groups. Normalized distances between pure odors and mixture were
357 obtained by dividing their EDs by the ED between the pure compounds NNL and HEX within each
358 group. The reliability of the EDs calculated on these large-dimension samples was assessed via
359 bootstrap resampling with replacement ($N=1000$ repetitions). The sampling distribution of
360 differences between two EDs was then tested by a z-test against a standard normal distribution
361 (after confirming its normality). A similar procedure was used to compare the ratios of the EDs. The
362 ratio distributions were obtained by bootstrapping ($N=1000$ repetitions), and each sampling
363 distribution of differences between ratios was tested by a z-test against a standard normal
364 distribution (after confirming its normality).

365 To visualize the response dynamics, the odor coding space dimension was reduced via a principal
366 component analysis (PCA) of the joint coding space of all three groups. Original data dimension
367 contains 486 variables (162 glomeruli \times 3 odors) and 180 samples (20 time points \times 3 trials \times 3
368 groups). Averaging over trials, groups, and the period 200-400 ms after stimulus onset provides

the transformation matrix for the PCA. The first two principal components explain respectively 76.75% and 23.25% of the overall variation. The average odor dynamics within in each group was then quantified by bootstrapping ($N = 1000$ repetitions) subsets of $n = 44$ glomeruli (the lowest n of active glomeruli, recorded in NNL pre-exposed bees) belonging to each treatment group. Then, the weighted components relative to each group were averaged across N and across all time points. The bootstrapping procedure was used to obtain balanced representations within the joint coding space even if number of original coding dimensions were different across groups. Single glomerular responses of T1-33 and T1-17 to the odor stimuli were compared among treatment groups via one-way ANOVA and independent sample t -tests. All pre-processing steps and analyses were conducted in MATLAB.

379

Brain dissociation and immunohistochemistry

After 72 h of odor exposure, a subset of bees was sacrificed, and brains were dissociated and processed for immunohistochemistry. Briefly, bees were decapitated and heads were fixed in a 4% paraformaldehyde solution (4 °C O/N). Brains were later carefully dissociated in PBS. Subsequent washing and immunostaining procedures were all conducted in a 0.5% Triton X-100 PBS solution. After blocking of non-specific sites through incubation in a 5% normal goat serum solution (1 h RT), the brains were incubated (48 h, 4 °C, 4% in Triton-PBS) with anti-synapsin antibodies (DSHB Hybridoma Product 3C11 (anti SYNORF1)). The binding sites were then revealed with an Alexa Fluor 546 secondary fluorescent antibody (Alexa Fluor 546 donkey anti-mouse IgG (H+L), Invitrogen Molecular Probes; incubation 48 h, 4 °C, 2% in Triton-PBS).

390

Optical imaging setup

Both morphological and functional images were acquired via two-photon microscopy (Ultima IV, Prairie Technologies-Bruker), equipped with an ultra-short pulsed laser (Mai Tai Deep See HP, Spectra-Physics-Newport) as excitation source. Excitation wavelength was 800 nm, fluorescence was separated by a dichroic beam-splitter, filtered by a 70 nm bandpass filter centered at 525 nm

396 (both Chroma), and detected by Photomultiplier tubes (Hamamatsu Photonics). Excitation and
397 signal collection were performed in epi-fluorescence configuration via a water-immersion objective
398 (20x, NA = 1, Olympus). Immersion liquid was Triton-PBS for *ex vivo* and Ringer's solution (Galizia
399 and Vetter 2004) for *in vivo* imaging.

400

401 Data analysis volumetric data

402 Z-stacks of the right and left ALs (3 μm step size along the anteroposterior axis) were evaluated in
403 ImageJ (Schneider et al. 2012), and glomeruli were identified. In cases where both the right and
404 the left sides were perfectly intact and unambiguous labelling of the glomeruli could be achieved,
405 the images were processed in Amira (FEI-Thermo Fisher Scientific) for 3D reconstruction and
406 volumetric measurements of the glomeruli of interest. The whole procedure was conducted blindly
407 with respect to both group and side, necessitating prior horizontal flipping of z-stacks of the right
408 AL.

409 Volumes were analyzed via a mixed ANOVA with side and glomerulus as within-subject factors
410 and treatment as between-subject factor. Each glomerulus was then analyzed via a repeated-
411 measure ANOVA with side as within-subject factor and treatment as between-subject factor.
412 Independent sample *t*-test comparisons were performed within each glomerulus, using a right-left
413 averaged measure of each glomerulus in each bee. All analyses were conducted in MATLAB.

414

415

416 Acknowledgements

417 We acknowledge financial support by the Autonomous Province of Trento, (Research unit IBRAIM)
418 and the Autonomous Province of Bolzano (project B26J16000310003).

419

420 References

421 Arenas A, Giurfa M, Sandoz JC, et al (2012) Early olfactory experience induces structural changes
422 in the primary olfactory center of an insect brain. *Eur J Neurosci* 35:682–90. doi:

423 10.1111/j.1460-9568.2012.07999.x

424 Brown SM, Napper RM, Mercer AR (2004) Foraging experience, glomerulus volume, and synapse
425 number: A stereological study of the honey bee antennal lobe. *J Neurobiol* 60:40–50. doi:
426 10.1002/neu.20002

427 Chakroborty NK, Menzel R, Schubert M (2016) Environment specific modulation of odorant
428 representations in the honeybee brain. *Eur J Neurosci*. doi: 10.1111/ejn.13438

429 Chandra SBC, Wright GA, Smith BH (2010) Latent inhibition in the honey bee, *Apis mellifera*: Is it a
430 unitary phenomenon? *Anim Cogn* 13:805–15. doi: 10.1007/s10071-010-0329-6

431 Chen J-Y, Marachlian E, Assisi C, et al (2015) Learning Modifies Odor Mixture Processing to
432 Improve Detection of Relevant Components. *J Neurosci* 35:179–197. doi:
433 10.1523/JNEUROSCI.2345-14.2015

434 Claudianos C, Lim J, Young M, et al (2014) Odor memories regulate olfactory receptor expression
435 in the sensory periphery. *Eur J Neurosci* 39:1642–1654. doi: 10.1111/ejn.12539

436 Colbert HA, Bargmann CI (1995) Odorant-Specific Adaptation Pathways Generate Olfactory
437 Plasticity in *C. elegans*. *Neuron* 14:803–812.

438 Das S, Sadanandappa MK, Dervan A, et al (2011) Plasticity of local GABAergic interneurons
439 drives olfactory habituation. *Proc Natl Acad Sci U S A* 108:E646-54. doi:
440 10.1073/pnas.1106411108

441 Deisig N, Giurfa M, Lachnit H, Sandoz J-C (2006) Neural representation of olfactory mixtures in the
442 honeybee antennal lobe. *Eur J Neurosci* 24:1161–74. doi: 10.1111/j.1460-9568.2006.04959.x

443 Denker M, Finke R, Schaupp F, et al (2010) Neural correlates of odor learning in the honeybee
444 antennal lobe. *Eur J Neurosci* 31:119–33.

445 Devaud J-M, Acebes A, Ramaswami M, Ferrús A (2003) Structural and functional changes in the

446 olfactory pathway of adult *Drosophila* take place at a critical age. *J Neurobiol* 56:13–23. doi:
447 10.1002/neu.10215

448 Devaud JM, Acebes A, Ferrús A (2001) Odor exposure causes central adaptation and
449 morphological changes in selected olfactory glomeruli in *Drosophila*. *J Neurosci* 21:6274–82.

450 Faber T, Joerges J, Menzel R (1999) Associative learning modifies neural representations of odors
451 in the insect brain. *Nat Neurosci* 2:74–8. doi: 10.1038/4576

452 Fernández VM, Arenas A, Farina WM (2009) Volatile exposure within the honeybee hive and its
453 effect on olfactory discrimination. *J Comp Physiol A Neuroethol Sens Neural Behav Physiol*
454 195:759–68. doi: 10.1007/s00359-009-0453-4

455 Fernandez VM, Giurfa M, Devaud J-M, Farina WM (2012) Latent inhibition in an insect: The role of
456 aminergic signaling. *Learn Mem* 19:593–597. doi: 10.1101/lm.028167.112

457 Frasnelli E, Haase A, Rigosi E, et al (2014) The Bee as a Model to Investigate Brain and
458 Behavioural Asymmetries. *Insects* 5:120–138. doi: 10.3390/insects5010120

459 Galizia GC, Vetter RS (2004) *Methods in Insect Sensory Neuroscience*. CRC press, Boca Raton

460 Giurfa M, Sandoz J-C (2012) Invertebrate learning and memory: Fifty years of olfactory
461 conditioning of the proboscis extension response in honeybees. *Learn Mem* 19:54–66. doi:
462 10.1101/lm.024711.111

463 Haase A, Rigosi E, Frasnelli E, et al (2011) A multimodal approach for tracing lateralisation along
464 the olfactory pathway in the honeybee through electrophysiological recordings, morpho-
465 functional imaging, and behavioural studies. *Eur Biophys J* 40:1247–58. doi: 10.1007/s00249-
466 011-0748-6

467 Haase A, Rigosi E, Trona F, et al (2010) In-vivo two-photon imaging of the honey bee antennal
468 lobe. *Biomed Opt Express* 2:131–8. doi: 10.1364/BOE.1.000131

469 Hourcade B, Perisse E, Devaud J-M, Sandoz J-C (2009) Long-term memory shapes the primary
470 olfactory center of an insect brain. *Learn Mem* 16:607–615. doi: 10.1101/lm.1445609

471 Linster C, Sachse S, Galizia CG (2005) Computational modeling suggests that response properties
472 rather than spatial position determine connectivity between olfactory glomeruli. *J Neurophysiol*
473 93:3410–7. doi: 10.1152/jn.01285.2004

474 Locatelli FF, Fernandez PC, Villareal F, et al (2013) Nonassociative plasticity alters competitive
475 interactions among mixture components in early olfactory processing. *Eur J Neurosci* 37:63–
476 79. doi: 10.1111/ejn.12021

477 Manning A (1967) “Pre-imaginal” conditioning in *Drosophila*.

478 Matsumoto Y, Menzel R, Sandoz J-C, Giurfa M (2012) Revisiting olfactory classical conditioning of
479 the proboscis extension response in honey bees: a step towards standardized procedures. *J*
480 *Neurosci Methods* 211:159–167. doi: 10.1016/j.jneumeth.2012.08.018

481 Paoli M, Androne M, Haase A (2017) Imaging Techniques in Insects. In: Rogers LJ, Vallortigara G
482 (eds) *Lateralized brain functions*, 1st edn. Springer New York, New York, NY, pp 471–519

483 Paoli M, Anesi A, Antolini R, et al (2016a) Differential Odour Coding of Isotopomers in the
484 Honeybee Brain. *Sci Rep* 6:21893. doi: 10.1038/srep21893

485 Paoli M, Weisz N, Antolini R, Haase A (2016b) Spatially resolved time-frequency analysis of odour
486 coding in the insect antennal lobe. *Eur J Neurosci* 44:2387–2395. doi: 10.1111/ejn.13344

487 Peele P, Ditzen M, Menzel R, Galizia CG (2006) Appetitive odor learning does not change
488 olfactory coding in a subpopulation of honeybee antennal lobe neurons. *J Comp Physiol A*
489 192:1083–103. doi: 10.1007/s00359-006-0152-3

490 Rath L, Galizia GC, Szyszka P (2011) Multiple memory traces after associative learning in the
491 honey bee antennal lobe. *Eur J Neurosci* 34:352–360. doi: 10.1111/j.1460-9568.2011.07753.x

492 Rigosi E, Frasnelli E, Vinegoni C, et al (2011) Searching for anatomical correlates of olfactory
 493 lateralization in the honeybee antennal lobes: a morphological and behavioural study. *Behav*
 494 *Brain Res* 221:290–294. doi: 10.1016/j.bbr.2011.03.015

495 Sachse S, Galizia CG (2002) Role of inhibition for temporal and spatial odor representation in
 496 olfactory output neurons: a calcium imaging study. *J Neurophysiol* 87:1106–17.

497 Sachse S, Rueckert E, Keller A, et al (2007) Activity-dependent plasticity in an olfactory circuit.
 498 *Neuron* 56:838–50. doi: 10.1016/j.neuron.2007.10.035

499 Sandoz J-C, Galizia CG, Menzel R (2003) Side-specific olfactory conditioning leads to more
 500 specific odor representation between sides but not within sides in the honeybee antennal
 501 lobes. *Neuroscience* 120:1137–1148. doi: 10.1016/S0306-4522(03)00384-1

502 Sandoz JC (2011) Behavioral and neurophysiological study of olfactory perception and learning in
 503 honeybees. *Front Syst Neurosci* 5:98. doi: 10.3389/fnsys.2011.00098

504 Schneider CA, Rasband WS, Eliceiri KW (2012) NIH Image to ImageJ: 25 years of image analysis.
 505 *Nat Methods* 9:671–675. doi: 10.1038/nmeth.2089

506 Sigg D, Thompson CM, Mercer AR (1997) Activity-dependent changes to the brain and behavior of
 507 the honey bee, *Apis mellifera* (L.). *J Neurosci* 17:7148–56.

508 Silbering AF, Galizia CG (2007) Processing of odor mixtures in the *Drosophila* antennal lobe
 509 reveals both global inhibition and glomerulus-specific interactions. *J Neurosci* 27:11966–77.
 510 doi: 10.1523/JNEUROSCI.3099-07.2007

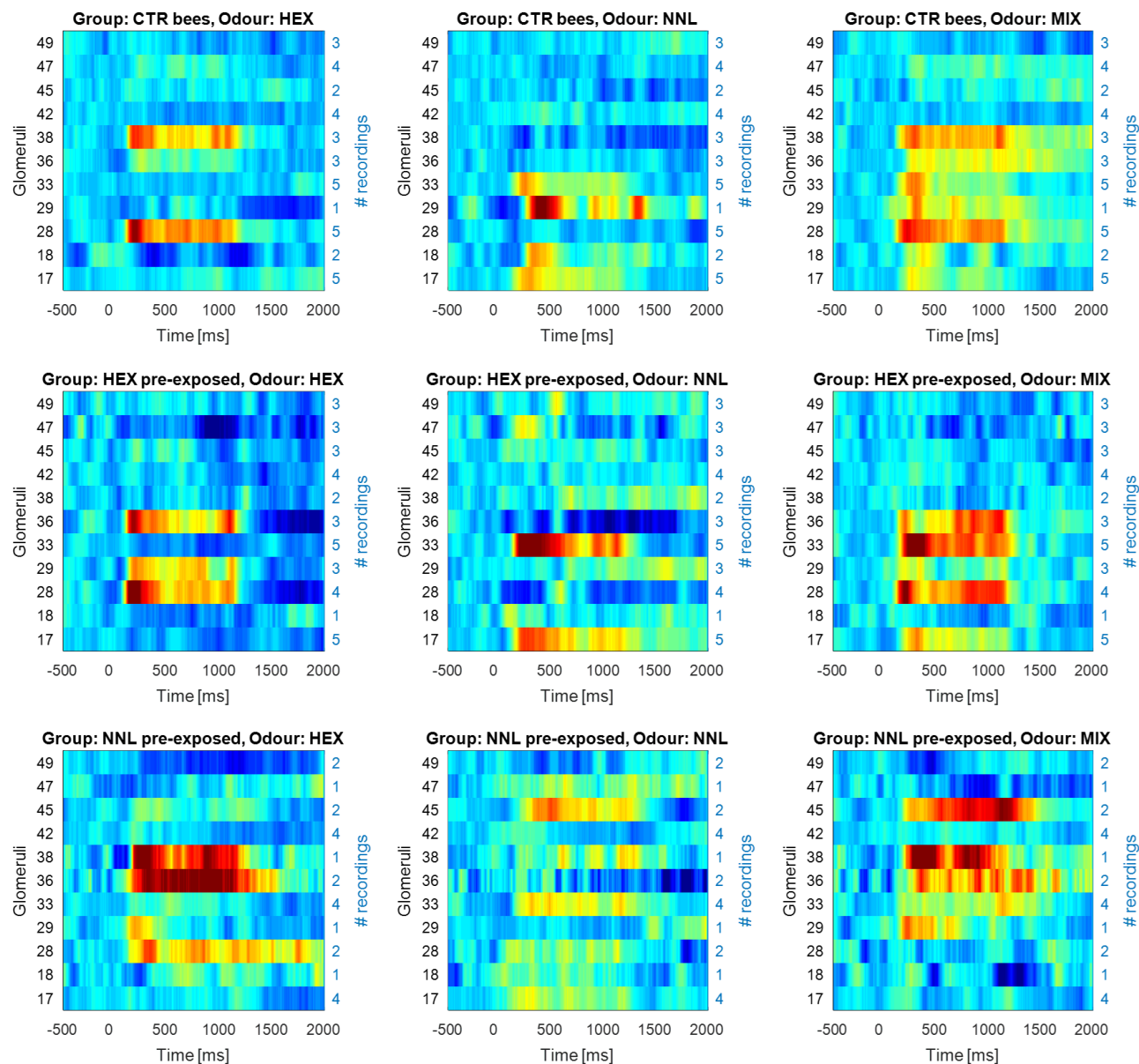
511 Sinakevitch IT, Smith AN, Locatelli F, et al (2013) *Apis mellifera* octopamine receptor 1 (AmOA1)
 512 expression in antennal lobe networks of the honey bee (*Apis mellifera*) and fruit fly
 513 (*Drosophila melanogaster*). *Front Syst Neurosci* 7:70. doi: 10.3389/fnsys.2013.00070

514 Sudhakaran IP, Holohan EE, Osman S, et al (2012) Plasticity of recurrent inhibition in the
 515 *Drosophila* antennal lobe. *J Neurosci* 32:7225–31. doi: 10.1523/JNEUROSCI.1099-12.2012

516 Winnington AP, Napper RM, Mercer AR (1996) Structural plasticity of identified glomeruli in the
517 antennal lobes of the adult worker honey bee. J Comp Neurol 365:479–90. doi:
518 10.1002/(SICI)1096-9861(19960212)365:3<479::AID-CNE10>3.0.CO;2-M

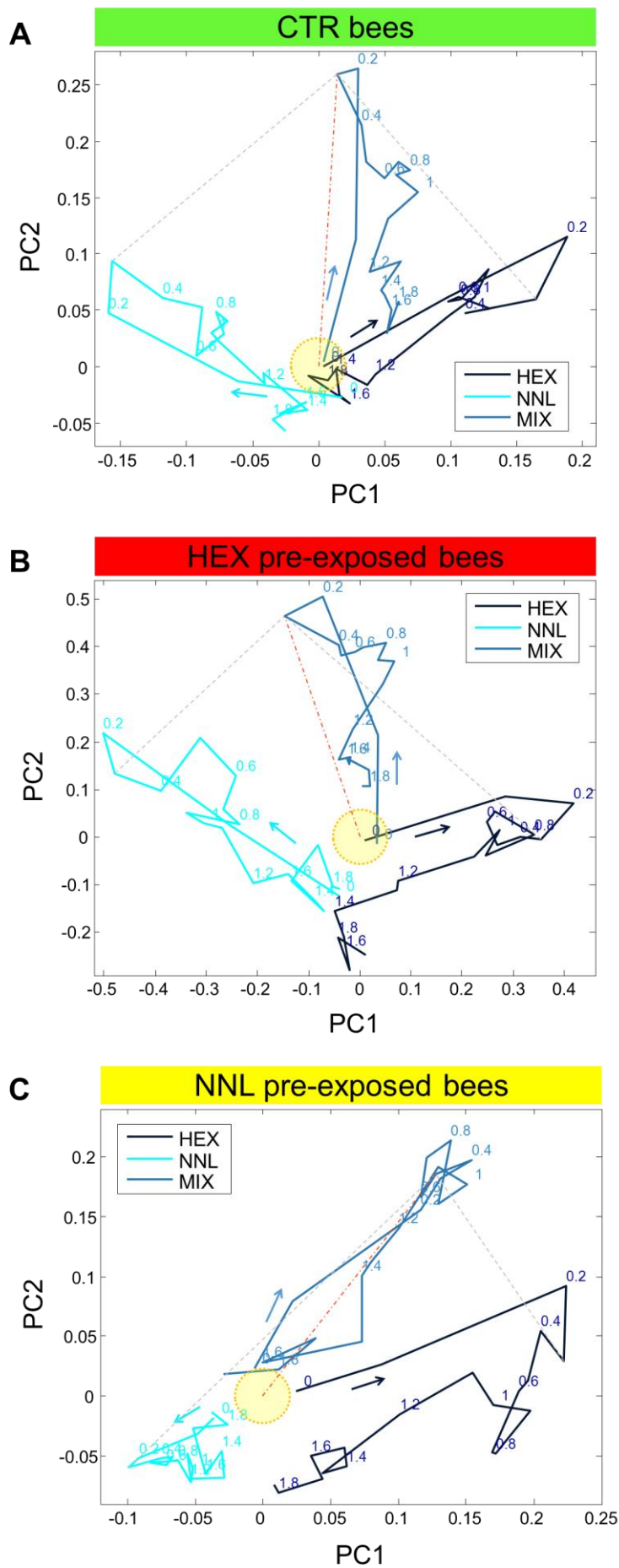
519 Zufall F, Leinders-Zufall T (2000) The cellular and molecular basis of odor adaptation. Chem
520 Senses 25:473–81. doi: 10.1093/CHEMSE/25.4.473

521



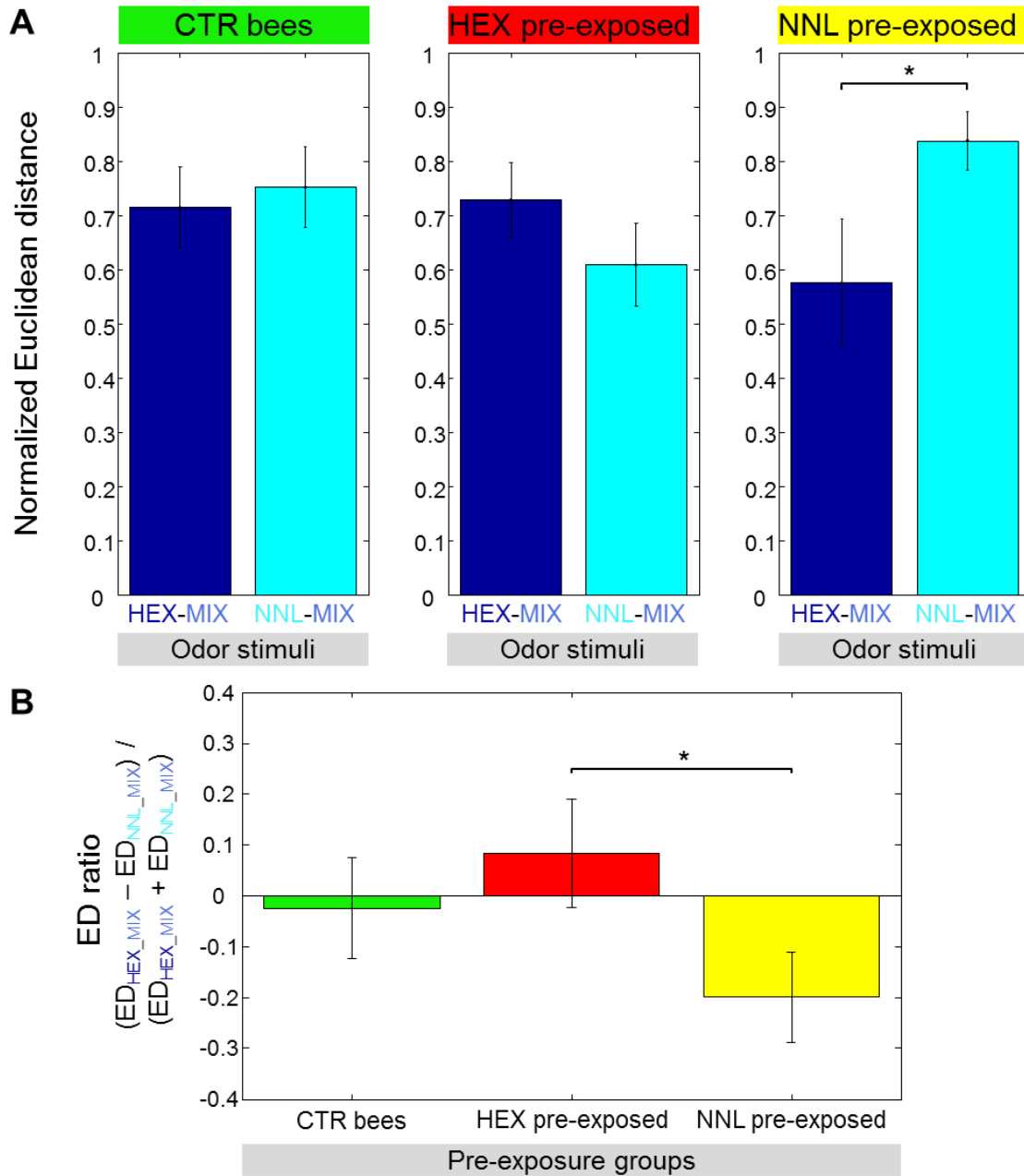
523

524 Figure 1: Fluorescence response maps of single glomeruli that were identified in at least one
525 subject per group, averaged over subjects. Shown are background subtracted and normalized
526 signals as a function of time from stimulus onset. The colormap reaches from inhibitive -0.1 (blue)
527 to activated +0.2 (red). Figures within rows are responses to different odors within the same pre-
528 exposed group. Columns show responses to the same odors in differently pre-exposed groups.
529 The right y-axis shows in blue the number of subjects in which the glomerulus was identified and
530 which therefore contributed to the averaging.



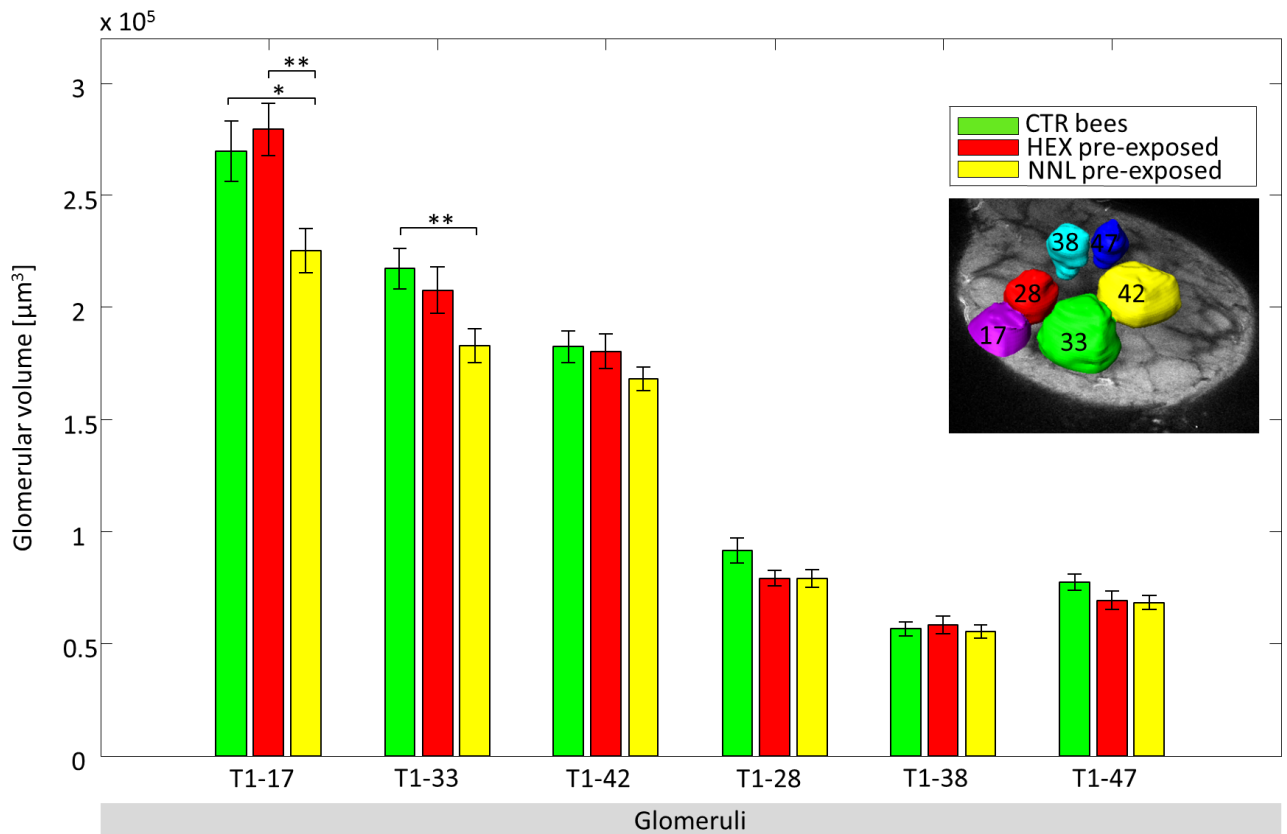
532 Figure 2: Activation dynamics during the presentation of three odor stimuli in the principal
533 component coordinate system (1 s stimulus and 1 s post-stimulus) for the 3 groups: (A) Control
534 (CTR) bees, (B) Hexanol (HEX) pre-exposed bees and (C) Nonanol (NNL) pre-exposed bees.
535 Activation vectors represent all measured glomeruli in a given treatment group. HEX activation
536 vector is shown in blue, NNL in cyan, and their binary mixture (MIX) in light blue. The origin,
537 marked by a yellow circle, corresponds to baseline activation. Arrows show the temporal axis;
538 numbers indicate time after stimulus onset in seconds. Dashed grey lines connect the 300 ms
539 time-points, which are the points of maximal odor separation. A dotted and dashed orange line
540 connects the origin with the binary mixture 300 ms time-point.

541



542

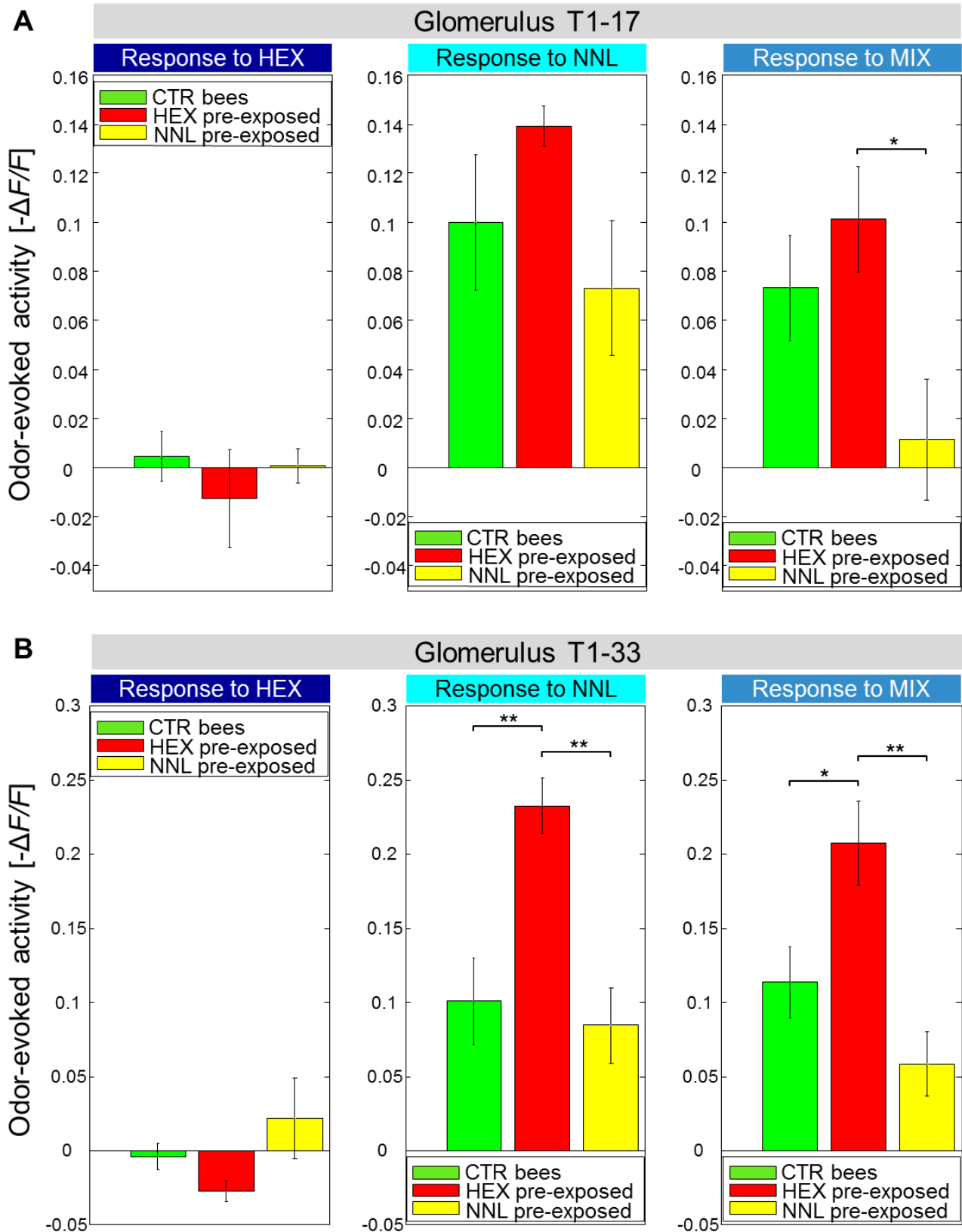
543 Figure 3: (A) Euclidean distances between representations of MIX and pure compounds within
 544 each group, normalized to the ED between the two pure compounds. Error bars represent
 545 standard deviations obtained via bootstrap resampling with replacement of glomeruli ($N = 1000$).
 546 The difference was significant in the NNL pre-exposed group (z-test, *: $p = 0.019$). (B) Ratios of
 547 normalized EDs $[(ED_{\text{HEX_MIX}} - ED_{\text{NNL_MIX}}) / (ED_{\text{HEX_MIX}} + ED_{\text{NNL_MIX}})]$ within each group. Error bars
 548 represent standard deviations obtained by bootstrapping. The shift between the HEX and the NNL
 549 pre-exposed groups was significant (z-test, *: $p = 0.041$).



550

551 Figure 4: The average volumes of the six glomeruli in the three treatment groups (CTR bees, HEX
 552 pre-exposed, and NNL pre-exposed bees). An example of segmented and 3D-reconstructed
 553 glomeruli T1-17, 33, 42, 28, 38, 47 from an immunolabelled left AL image stack is shown in the
 554 inset. Volume data were obtained by left-right averaging (see Materials and Methods). Error bars
 555 represent standard errors of the mean ($n_{\text{CTR}} = 13$, $n_{\text{HEX}} = 15$, $n_{\text{NNL}} = 15$). Groups with significantly
 556 different means are indicated (*: $p < 0.05$, **: $p < 0.01$).

557



558

559 Figure 5: Odor-evoked activity of glomeruli T1-17 (A) and T1-33 (B) in the three treatment groups,

560 averaged over single bees. Error bars represent standard errors of the mean ($n_{\text{CTR}} = 5$, $n_{\text{HEX}} = 5$,

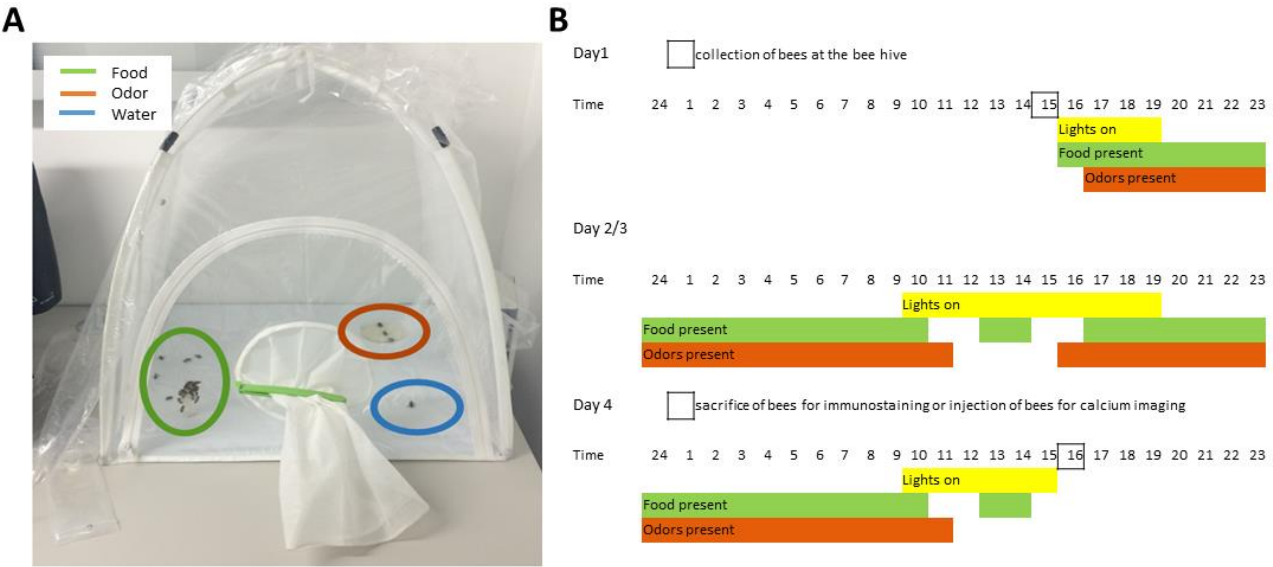
561 $n_{\text{NNL}} = 4$). The left histograms show the responses to 1-hexanol of all three treatment groups; the
562 middle histograms, to 1-nonanol; and the right histograms, to the 50:50 mixture. The treatment
563 effect was found to be significant via one-way ANOVA, and group means were confronted via two-
564 sample t -tests (*: $p < 0.05$, **: $p < 0.01$).

565

566 **Supplementary material**

567

568 **Supplementary Figure 1**



569

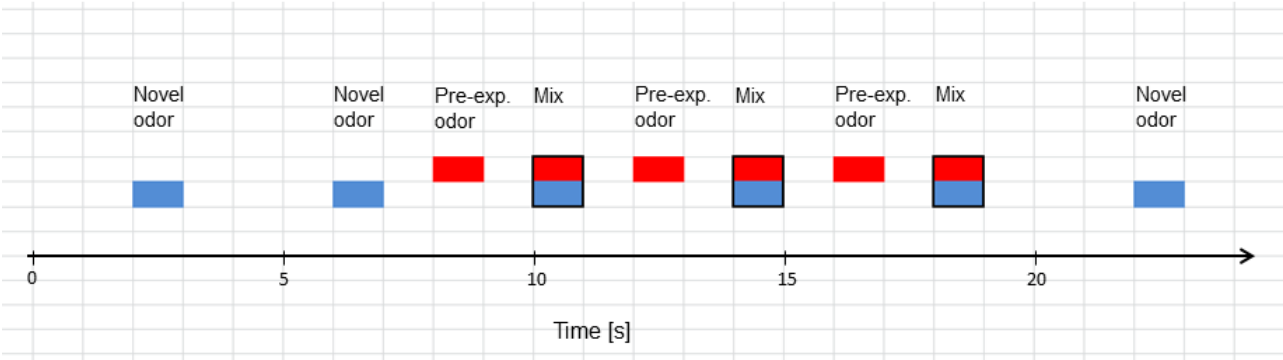
570 Figure S1: A) Bee tent used for odor exposure. Circled in green, orange and blue are,
571 respectively: the sucrose solution-containing Boardman bottle, the odor stimulus, water. B) Daily
572 schedule of odor/food/light exposure. Bees were initially provided with food and water. The odor
573 dispenser was added after one hour. Each following day, food and odors were removed
574 independently for certain periods, according to the schedule, and renewed afterwards. After 72h,
575 bees were either sacrificed for immunostaining, or injected with fura-2 for calcium imaging. After
576 injection, bees were placed back into the tents overnight for dye diffusion. They were finally
577 removed from tents in the next morning, a few hours before the imaging experiments.

578

579

580

581 Supplementary Figure 2

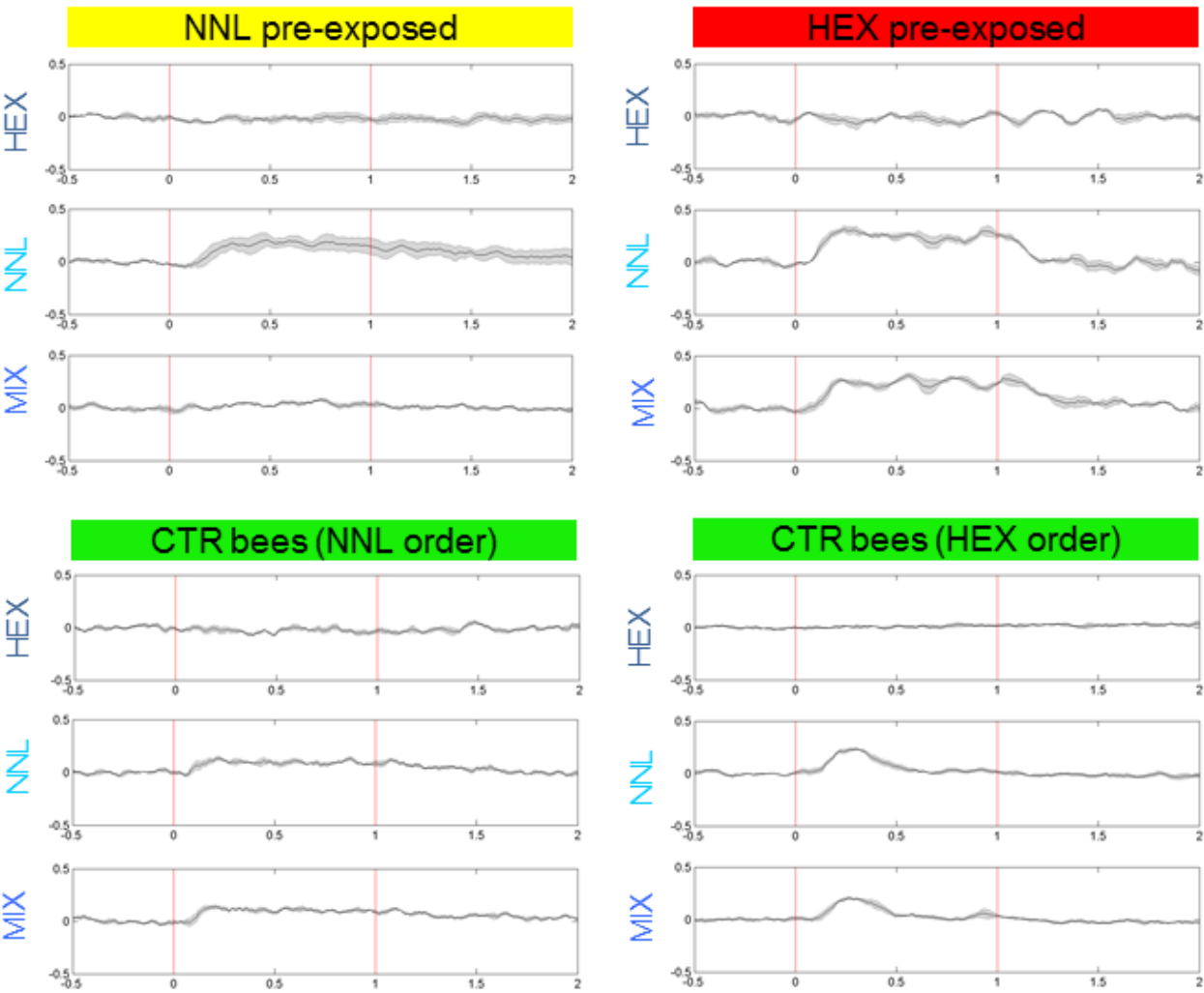


582
583 Figure S2: Paradigm of odor stimulation delivered to the bee antennae through a stimulus
584 generator. Each stimulus had duration 1 s. The initial delay was 2 s for the novel odor and 8 s for
585 pre-exposed odor. By using stimulus periods of 4 s for the novel odor and 2 s for the pre-exposed
586 odor, a stimulus pattern is created which presents the novel odor, the pre-exposed odor and the
587 binary mixture in a pseudo-random manner. CTR bees underwent the exposure protocol of either
588 HEX or NNL pre-exposed bees by random choice.

589

590

Glomerulus T1-33 odour-evoked responses.



592

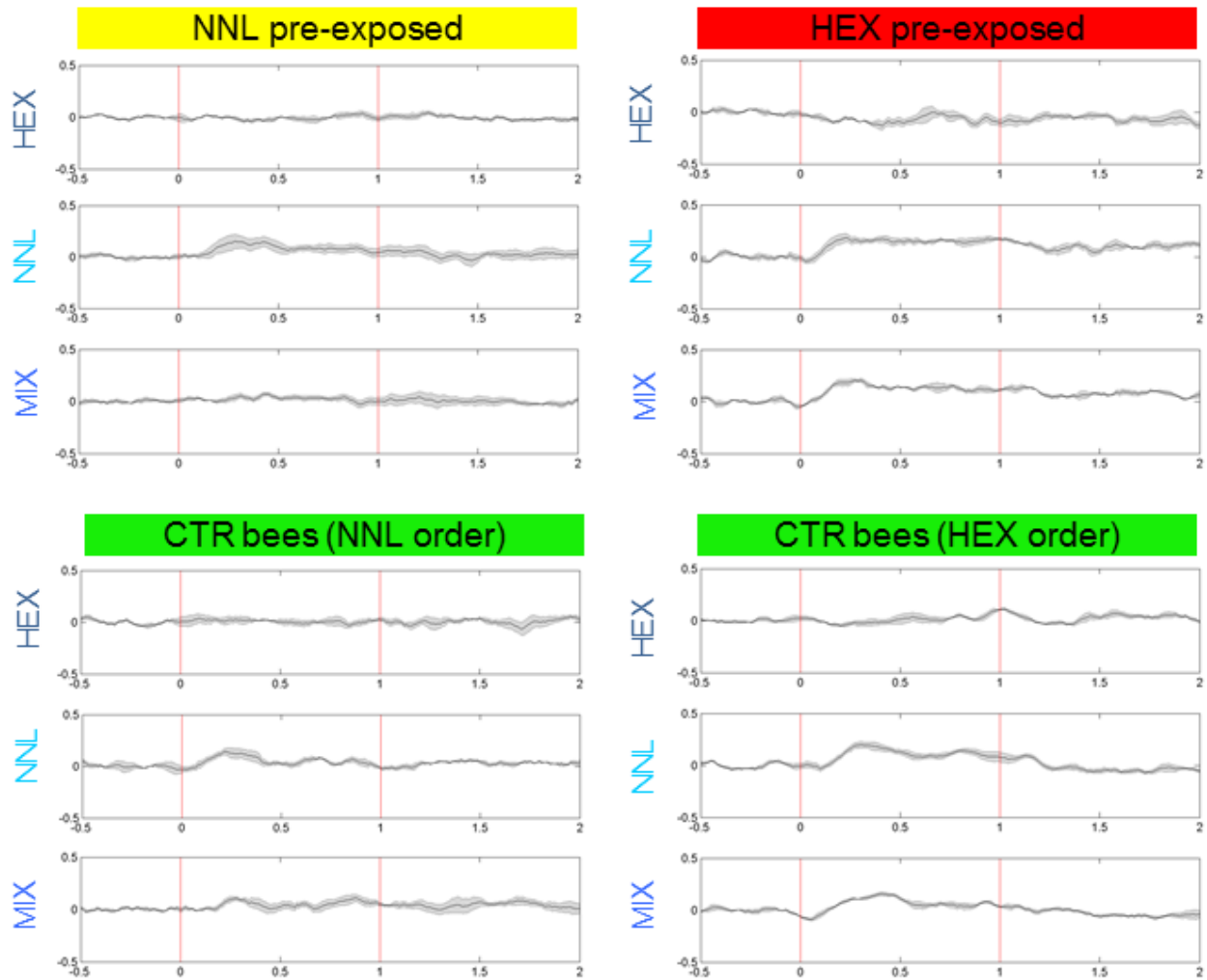
593 Figure S3: Odor evoked response $[-\Delta F/F]$ of glomerulus T1-33 recorded under different stimulation
594 paradigms. Four glomeruli T1-33 of four example bees are presented (one NNL pre-exposed bee,
595 one HEX pre-exposed bee, and two CTR bees, which were subjected to either the stimulation
596 paradigm of NNL pre-exposed bees or to that of HEX pre-exposed bees). The response to the
597 three odors shows a pattern that is typical of the treatment group and not of the “order” group. In
598 particular, in CTR and HEX pre-exposed bees, the profile response to 1-nonanol (NNL) is found
599 almost unchanged in the response to the binary mixture (MIX). In NNL pre-exposed bees,
600 response to binary mixture is flat, as it is the one to 1-hexanol. The plots represent three odors
601 repetitions averaged \pm SEM (shadow). Red vertical bars represent odors onset and offset.

602

603

604

Glomerulus T1-17 odour-evoked responses.



606

607 Figure S4: Odor evoked response $[-\Delta F/F]$ of glomerulus T1-17 recorded under different stimulation
608 paradigms. Four glomeruli T1-17 of four example bees are presented (one NNL pre-exposed bee,
609 one HEX pre-exposed bee, and two CTR bees, which were subjected to either the stimulation
610 paradigm of NNL pre-exposed bees or to that of HEX pre-exposed bees). The response to the
611 three odors shows a pattern that is typical of the treatment group and not of the “order” group. In
612 particular, in CTR and HEX pre-exposed bees, the profile response to 1-nonanol (NNL) is found
613 almost unchanged in the response to the binary mixture (MIX). In NNL pre-exposed bees,
614 response to binary mixture is flat, as it is the one to 1-hexanol. The plots represent three odors
615 repetitions averaged \pm SEM (shadow). Red vertical bars represent odors onset and offset.

616

617